

Experimental Determination of Composite Stacking Sequence Using Four Point Bend Test

ME EN 6960

Nik Benko, John Callaway, Nick Dorsett, Martin Raming

February 26, 2018

Abstract

There are several different techniques to determine ply orientations within a composite laminate (stacking sequence). In this experiment we utilized laminated plate theory (LPT) with experimental techniques in order to determine the correct stacking sequence of a composite laminate. We were provided a list of five possible stacking sequences for a composite panel in question. This panel was made of T800-3900 carbon fiber prepreg. LPT can be used to predict either stresses or strains of a composite laminate if given material properties, forces, and a stacking sequence. In this project we utilized LPT to predict strains for loading conditions that would match mechanical testing. Our mechanical testing consisted of a four-point bend test to induce a known moment in mid-section of our composite specimen. By attaching 3 strain gauges to the mid-section we recorded strains during mechanical testing. We then compared and best matched recorded strains to calculated strains to determine the correct stacking sequence. Verification was done through polishing and visual inspection of a side of the composite laminate. A four point bend test was used to determine the layup of a composite laminated plate

1 Introduction

Composite materials are currently used in many applications where a high stiffness to weight ratio is important for design and operations such as in the aerospace and sports industries. While the idea of using combined materials to improve the capability of a structure has been utilized for thousands of years, use of modern composites like carbon fiber with an epoxy matrix is a relatively new practice. As the industry first began many questions developed involving engineering design implications such as failure criteria and material response. The main challenge for modern composites is the orthotropic nature of the material. Modern composite lamina tend to have a significantly larger Young's modulus in the fiber direction compared to the matrix direction. This orthotropic property is also what makes composites desirable when designing a structure that requires different material responses relative to global orientation. This is done by stacking individual plies in different orientations with respect to each other to create a laminate. The way in which these plies are oriented is also known as a stacking sequence.

To analytically understand how a stacking sequence of a laminate responds to a loading condition we turn to laminated plate theory (LPT). LPT first evolved in the 1950's and 60's.[?] The theory relies on the material properties in the material coordinates system, stacking sequence, and ply thickness to arrive at what is know as the ABD matrix. The ABD matrix can then be used to solve for strains, curvatures and stresses for a given load vector containing forces and moments. The ABD matrix is a 6×6 matrix comprised of 36 components which makes for difficult hand calculations. For this reason it is often convenient to utilize a coding software to perform calculations as was done in this experiment.

LPT has proven to be very useful in design considerations but can be used for other purposes. In this report we explore the use and accuracy of LPT to back out a stacking sequence by comparing calculated results to experimental results. The goal of this experiment is to find which of the five unique laminate stacking sequence given matches the configuration of the specimen in question. In order to get data for comparison we loaded our specimen at intervals in a four-point bend flexure device while recording strains using strain gauges. We potentially only needed one induced moment but performed several for completeness and accuracy.

In this report we start by further expanding on LPT and implications of using the theory. We then discuss the experimental techniques and performed procedures used to arrive at force induced strains of our specimen. Possible errors and uncertainties relating to the experiment are then considered at the end of the methods section. Results are presented and discussed in the preceding our conclusion. All figures and tables can be located in section seven.

2 Methods

2.1 Laminated Plate Theory

The composite materials used in this lab are classified as specially orthotropic materials, meaning that they have the same material constants in two directions and differ in the third. This also means that four independent material constants are required to define the material stiffness. The constants used are E_1 , the stiffness in the fiber direction, E_2 , the stiffness 90 degrees from the fiber direction, G_{12} , the shear modulus in the 1-2 plane, and ν_{12} , Poisson's ratio defining strain in the 2 direction due to applied force in the 1 direction. These material constants are used in Equation 1 to define the material stiffness matrix Q . This matrix in the 3×3 form shown assumes plane stress conditions, it was reduced from its 6×6 form by ignoring all z-direction stresses. This Q matrix is only applicable for a single ply with its fibers aligned in the x-direction. Tensor transformations can be used to apply stiffnesses in any orientation desired. Equation 2 shows the transformation matrix of sine and cosine terms used to transform the matrix, and equation 4 is the equation used to actually apply the rotation, generating Q_{bar} , used to denote this transformed stiffness. It is important to note that the Reuter matrix, denoted R , is used because its factor of 2 is necessary to satisfy tensor rotation rules.

These stiffnesses are used to calculate material constants for single plies of material. Laminated Plate Theory (LPT) is used to compute matrices that relate forces, moments, strains, and curvatures. Using LPT requires the assumptions of perfectly bonded plies, plane sections remaining plane during deformation, thin laminates (length and width must be at least 10x

the thickness), small mid-plane displacements and rotations, plane stress conditions, and transverse stresses to be neglected. These conditions being satisfied, equations 5, 6, and 7 are used to calculate three matrices denoted A, B, and D based up on the Q_{bar} matrix for each individual ply and z, which is the distance of each ply interface from the mid-plane of the laminate. These are combined into a 6x6 matrix that relates mid-plane strains and curvatures with normal forces and moments. The A matrix relates normal forces with normal strains, the D matrix relates moments and curvatures, and the B matrix relates both normal forces with curvatures and moments with normal strains.

2.2 Experimental Techniques

2.2.1 Strain Analysis

Electrical strain gauges are a commonly used tool in engineering applications to accurately measure axial strain. The essential aspect of a strain gauge is made up of a very thin wire. Since the gauge is bonded to the surface of the material it extends or contracts with the specimen surface. This elongation or compression of the wires in the strain gauge causes the electrical resistance to change. Strain can then be determined by the fact that material deformation is dependent on material electrical resistivity. This relationship between resistivity and deformation of the given alloy in a strain gauge is referred to as the gauge factor (GF).

Electrical strain gauges are essentially a Wheatstone bridge which consists of four electrical resistors that act as two voltage dividers in parallel. There are three unique configurations that strain gauges can have depending on the number of active resistors in the Wheatstone bridge. These configurations are named full-bridge, half-bridge, and quarter-bridge of which contain four active elements, two active elements and one active element, respectfully. Additionally, the orientations of the active elements will determine the “type” of configuration. Testing setup, temperature differences, and type of strain to be measured dictates which configuration to use. In our experiment a quarter-bridge type I configuration was used for all strain gauges. This configuration was chosen since bending strain is to be measured and temperature effects will be negligible.

By applying a excitation voltage V_{EX} to the strain gauges we can measure then voltage beyond the active resistors V_{CH} . V_{CH} is typically very small so amplifiers are used in signal conditioning to boost signal levels. This aids in accuracy and resolution while reducing noise in the signal. Our amplification or $Gain$ is calculated in equation12 and is related to the V_{EX} and a scaling factor R_{shunt} related to a setting in the Dewetron oscilloscope used for voltage measurement. From there we can calculate our voltage ratio V_R with equation11 and finally plug into equation10 to convert voltage to strain.

Three strain gauges were implemented to measure strains near the mid section of the specimen. As figure ?? shows the strain gauges were oriented to achieve a 45° rosette. This type of strain rosette will allow for a direct measurement of strain in the lengthwise ϵ_x and strain in the crosswise direction ϵ_y . The shearing strain γ_{xy} can then be calculated using equation 9 where ϵ_{OB} is placed at a 45° from either the crosswise or lengthwise axes.

2.2.2 Mechanical Testing

A four-point flexure test was chosen as the best mechanical testing procedure. As Figure?? shows the resultant moment is constant in the specimen within the region between the two loading points. Since the strain gauges are also located in this region we can be certain the measured strain is caused by the moment induced by the load frame. For each load the moment in this region was calculated with equation 13, where P is the load, and L is the span. Because there is inevitably some initial compliance within the load frame we chose the first load increment to be above 45N to avoid false readings.

2.3 Procedure

To begin the lab section, groups were given a 3"x12" strip of a composite laminate to test. To prepare it for testing, strain gauges were attached. To accomplish this, the surface of a glass plate, the sample, and a pair of tweezers were degreased with acetone. Next, the surface of the composite sample was wet sanded using 320 grit sandpaper and M-Prep Conditioner A. After sanding the surface was wiped clean. A square was used to make alignment marks on the surface of the sample with a pencil, making marks at 0, 45, and 90 degrees. M-Prep Neutralizer 5A was applied and the surface was wiped in a single direction with a fiber-free paper. This was continued until the paper did not have any contaminants on it after wiping. Once the sample surface was clean, the strain gauge was removed from its plastic sleeve and placed on the cleaned glass surface, bonding side down. Tape was placed on top of the strain gauge and used to lift it off the surface at a 45 degree angle or less. The strain gauge was then transferred onto the composite sample with the alignment marks on the gauge matched up with the lines drawn earlier. Once lined up, the tape was partly peeled up allowing access underneath the gauge region. M-Bond 200 catalyst was applied to the gauge region by lifting the brush out of the bottle, wiping the brush ten times against the inside of the neck of the bottle, and then sliding the brush over the gauge region, wiping all the way outside of the gauge region before lifting the brush. The catalyst was then allowed to dry for one minute. Within 3-5 seconds, one or two drops of M-Bond 200 adhesive was applied to the base of the tape, outside the gauge region and the tape, with the strain gauge, was pressed down onto the surface with a wiping motion, starting with the base of the tape where the adhesive was placed and moving along the length of the tape. Gentle pressure was then applied onto the top of the strain gauge for at least one minute. Finally, the tape was removed by slowly peeling it directly back over itself. These steps were repeated twice more to attach all three strain gauges.

Following the attachment of the strain gauges, the lead wires from a Dewetron DEWE-30-8 were soldered to the terminals on the strain gauges by first priming the contacts with solder and then using a bead of solder to secure the wires to the terminals. The positive and negative terminal orientation did not matter. Once attached, the Wheatstone bridge corresponding to each gauge inside the DEWE-30-8 was balanced using the corresponding software, and the sample was gently flexed to ensure that the gauges were creating voltage differentials. Once everything was confirmed to be working, the sample was placed inside a four point bend fixture with the gauge region inside the load span on the fixture. Once everything was prepared, the sample was loaded at approximately 50 Newton increments. At each increment,

the load was determined and the oscilloscope which was used to take voltage measurements was paused. The voltage outputs from the strain gauges were then recorded. This process was repeated using 50N increments until 250N and then the last load step was 30N to avoid over-stressing the laminate. Following this, the load was removed from the sample, and the sample was flipped over inside the fixture. The loading process was repeated with the laminate in this configuration. Finally, using the relevant equations, the voltages were related to strains and the forces applied were transformed into moments thereby allowing a list of possible laminates to be iterated across using a Matlab script until a match was found for the stacking sequence.

2.4 Error and Uncertainties

For this experiment, there were two major sources of error and uncertainty. First was the alignment of the strain gauges. In order to get accurate in-plane strain measurements, the gauges in the rosette must be evenly spaced at 45° and aligned with the edges of the plate. Strain gauges placed by hand are inherently susceptible to mild misalignment. To quantify the deviation from 45° spacing, we imaged our plate after testing with a reference 90° angle and used ImageJ (NIH) to measure the angles between gauges. Figure (number) shows the image and corresponding alignment angles.

A second source of error came in the measurement of voltage. Voltage readings were taken by aligning the oscilloscope channel cursor with what was perceived to be the average of a voltage trace at a given time. As voltage increased, the sensitivity of the cursor decreased, limiting the ability to determine voltage to within more than 2-4% of the actual value. As a result, measurements of strain must also vary by $\pm 4\%$

3 Results

Material properties of T800-3900 (Table 1), potential ply orientations (Table 2) and collected experimental data (Table 3) were combined using the previously described procedure to produce actual strains and predicted strains for the five potential layups. Results for normal strains in the x and y directions, along with shear strain are presented in Table 4.

Comparison of actual and predicted values show that Layup 3 ($[(90)_2/(0)_4/(90)_2]_S$) was the composite laminate tested during the experimental process. Predicted vs. actual strains for this layup are presented in Figure 1.

4 Discussion

Determination of the ply orientation of the tested laminate was accomplished by eliminating potential stacking sequences from the provided list using a comparison of the actual measured strains with the predicted strains from laminated plate theory. Layups 2 and 5 were eliminated by thickness of the laminate and large predicted strains in the x-direction compared to actual x-direction strains. Layup 1 was eliminated by large predicted shear strain values compared

to actual shear strains. Layup 4 was eliminated by predicted positive shear strain compared to the actual negative shear strain seen during the experiment. This process resulted in the elimination of all layups with the exception of Layup 3

Although Layup 3 presented the best match of experimental and predicted strains, there are variations that can be seen, especially with the y-direction strains and the shear strains. As force was increased, the variation of actual strain and predicted strain increased. This can be explained by the errors in strain gauge orientation and voltage measurements described in the Error and Uncertainty section. This same error was not seen in the x direction, with actual values following the predicted values closely.

The variation seen in two of the three strain gauges shows one of the limitations of this method for determining stacking sequence. Since there is a potential for a high level of variation in strain measurements, this method is not sensitive to determining different stacking sequences that produce similar strain values. Also, this would provide potential prediction errors if a large number of stacking sequences are possible.

Another limitation of this method is that the possible stacking sequences must be known prior to performing the experiment. Carbon composite laminates provide an almost infinite number of potential stacking sequences. Even if the possible lamina orientations were limited to four (0,90,+45,-45), a 16 ply laminate (as was tested in this experiment) could have over 65,000 possible stacking sequences. It would be nearly impossible to eliminate all but one stacking sequence with the aforementioned error.

Despite the limitations of this method, it does effectively predict the stacking sequence of a carbon composite laminate when a small number of potential stacking sequences are known, and there is a large enough difference in the strain values predicted by laminated plate theory between these stacking sequences.

5 Conclusion

6 Figures

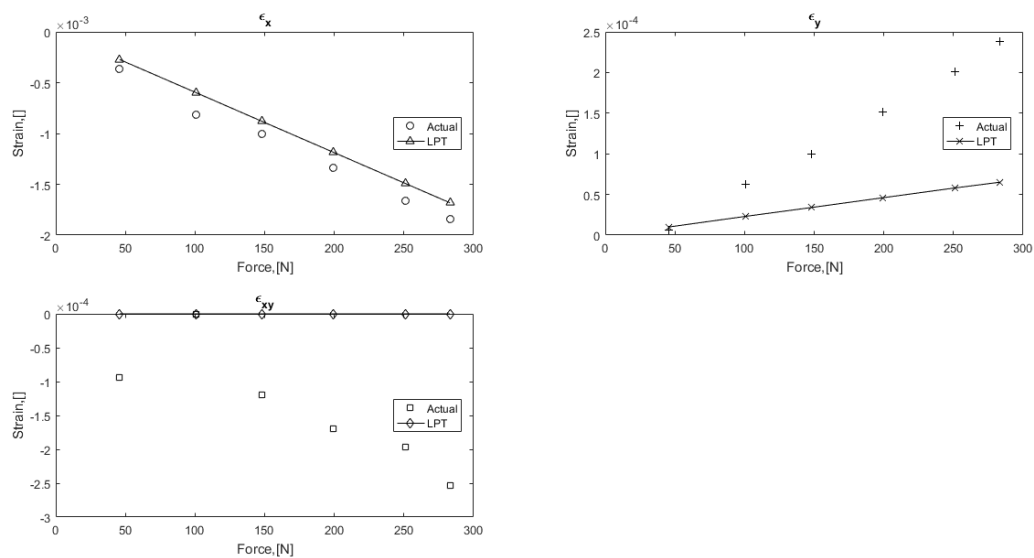


Figure 1: Force vs. Strain for Layup 3

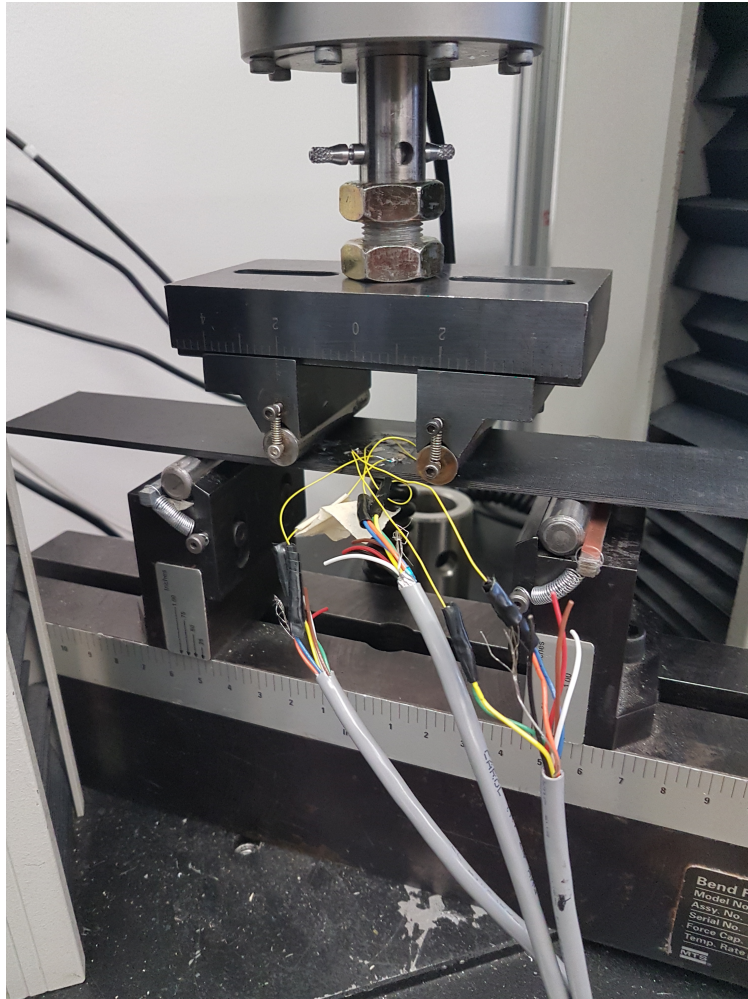


Figure 2: Mechanical test set up with four-point bend fixture

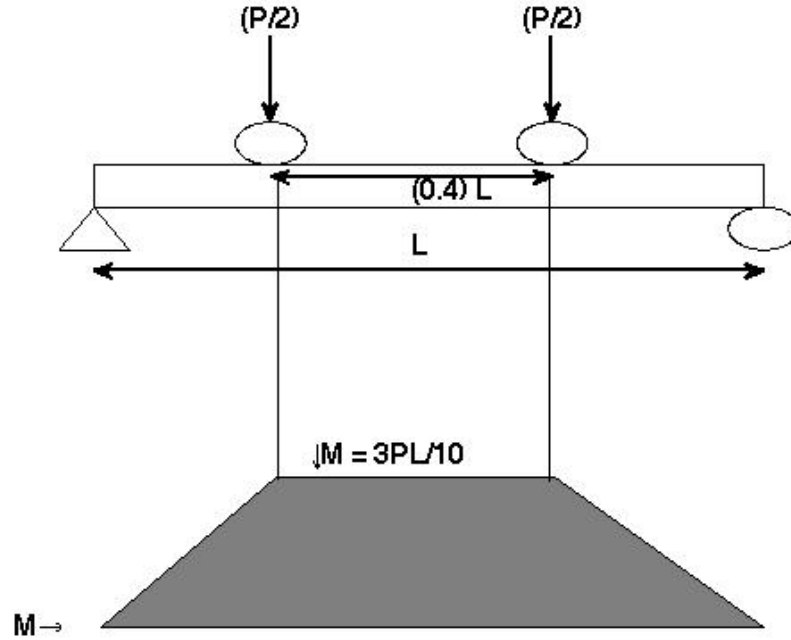


Figure 3: Moment diagram of four-point flexure setup used in mechanical testing.

7 Tables

Parameter	E_1	E_2	G_{12}	ν_{12}	ν_{21}
Value	114 GPa	8.3 GPa	3.93 GPa	0.33	0.02

Table 1: T800-3900 Material Properties

Layup #	Ply Orientation
1	$[(90/45/0/45)_2]_S$
2	$[45/90]_4$
3	$[(90)_2/(0)_4/(90)_2]_S$
4	$[90/45/0/-45]_4$
5	$[(90)_2/(0)_2]_2$

Table 2: Ply Orientation of Five Potential Layups

Specimen Data			Strain Gage Data		
Support Span:	0.127	(m)	Gage 1 Orientation:	90	(degrees)
Load Span:	0.0508	(m)	Gage 2 Orientation:	0	(degrees)
Length:	0.305	(m)	Gage 3 Orientation:	45	(degrees)
Width:	0.04925	(m)			
Thickness:	0.0028	(m)	Excitation Voltage:	12	(V)
			Gage Factor:	2.125	
			Dewetron Setting:	83.333	(mv/V)
			Calculated Gain:	5.00002	
Collected Load and Voltage Data					
Gages on Top:					
Load (N)	Gage 1 Voltage	Gage 2 Voltage	Gage 3 Voltage		
45.78	-0.0002	0.0116	0.0072		
100.5	-0.002	0.026	0.012		
148.3	-0.0032	0.0322	0.0164		
199.5	-0.0048	0.0426	0.0216		
251	-0.0064	0.053	0.0264		
283	-0.0076	0.0588	0.0296		
Gages on Bottom:					
Load (N)	Gage 1 Voltage	Gage 2 Voltage	Gage 3 Voltage		
55.98	0.0044	-0.0092	-0.0064		
104.7	0.006	-0.0196	-0.0124		
160.7	0.0072	-0.0316	-0.0196		
204.8	0.0084	-0.0396	-0.0252		
256.5	0.008	-0.049	-0.032		
279.1	0.0104	-0.053	-0.0352		

Table 3: Measured Data From Experimental Process

		ϵ_x				
		LPT Predicted				
Load (N)	Actual Strain	Layup 1	Layup 2	Layup 3	Layup 4	Layup 5
45.78	-0.000364	-0.000447	-0.004975	-0.000272	-0.000345	-0.001291
100.5	-0.000815	-0.000981	-0.010920	-0.000597	-0.000758	-0.002833
148.3	-0.001009	-0.001447	-0.016110	-0.000882	-0.001118	-0.004180
199.5	-0.001335	-0.001947	-0.021680	-0.001186	-0.001504	-0.005624
251	-0.001660	-0.002450	-0.027280	-0.001492	-0.001893	-0.007075
283	-0.001841	-0.002762	-0.030750	-0.001682	-0.002134	-0.007977

		ϵ_y				
		LPT Predicted				
Load (N)	Actual Strain	Layup 1	Layup 2	Layup 3	Layup 4	Layup 5
45.78	0.000006	0.000041	0.000418	0.000010	0.000092	-0.000048
100.5	0.000063	0.000089	0.000918	0.000023	0.000203	0.000104
148.3	0.000100	0.000131	0.001354	0.000034	0.000299	0.000154
199.5	0.000151	0.000177	0.001822	0.000046	0.000403	0.000207
251	0.000201	0.000222	0.002292	0.000058	0.000507	0.000261
283	0.000238	0.000251	0.002584	0.000065	0.000571	0.000294

		ϵ_{xy}				
		LPT Predicted				
Load (N)	Actual Strain	Layup 1	Layup 2	Layup 3	Layup 4	Layup 5
45.78	-0.000094	0.000308	0.003713	0.000000	0.000024	0.000000
100.5	0.000000	0.000675	0.008150	0.000000	0.000054	0.000000
148.3	-0.000120	0.000996	0.012030	0.000000	0.000079	0.000000
199.5	-0.000170	0.001340	0.016180	0.000000	0.000107	0.000000
251	-0.000196	0.001686	0.020360	0.000000	0.000134	0.000000
283	-0.000253	0.001901	0.022950	0.000000	0.000151	0.000000

Table 4: Predicted vs. Actual Strain Values for Potential Layups

8 Appendix

8.1 Code

```

1
2
3
4 % LPT Code
5 %Text inputs to inputs.txt
6 %Line 1 is material properties E1, E2, G12, v12
7 %Line 2 is strength for failure critereon
8 %Line 3 is thermal coefficients
9 %Line 4 is ply thickness
10 %Line 5 is ply orientation layup
11 %Line 6 is loading - N_x, N_y, N_xy, M_x, M_y, M_xy
12 %Line 7 is temperature change
13
14 clear , clc
15 format short g
16
17 F = csvread ('inputs.txt');
18 fileID = fopen('inputs.txt');
19 C = textscan(fileID, '%f %f %f %f %f %f %f %f %f %f %f %f %f %f %f'
    '%f %f %f %f %f %f %f', 'delimiter', ',');
20 fclose(fileID);
21
22 for k = 1:length(C)
23     ply(k) = C{k}(5);
24 end
25 ply(find(isnan(ply))) = [];
26
27 % Name constants from text file:
28 % Material properties:
29 E1 = F(1,1);
30 E2 = F(1,2);
31 G = F(1,3);
32 v = F(1,4);
33
34 % Strength Properties:
35 S_L_plus = F(2,1);
36 S_L_minus = F(2,2);
37 S_T_plus = F(2,3);
38 S_T_minus = F(2,4);
39 SLT = F(2,5);
40
41 % Coefficients of thermal expansion
42 alpha_1 = F(3,1);
43 alpha_2 = F(3,2);
44
45 % Ply thickness\
46 t = F(4,1);
47
48 % Laminate stacking

```

```

49 L = ply;
50
51 % Forces and moments
52 N_x = F(6,1);
53 N_y = F(6,2);
54 N_xy = F(6,3);
55 M_x = F(6,4);
56 M_y = F(6,5);
57 M_xy = F(6,6);
58
59 % Temperature change
60 Temp = F(7,1);
61
62 %1. Calculate Q and S matrices:
63
64 R = [1 0 0
65      0 1 0
66      0 0 2];
67
68 S = [1/E1 -v/E1 0
69      -v/E1 1/E2 0
70      0 0 1/G];
71
72 Q = inv(S);
73
74 % 1. Calculate Q_bar and S_bar matrices
75 for i = 1:length(L)
76     theta = L(i);
77
78     T = [(cosd(theta)).^2 (sind(theta)).^2 2*sind(theta).*cosd(theta)
79          (sind(theta)).^2 (cosd(theta)).^2 -2*sind(theta).*cosd(theta)
80          -sind(theta).*cosd(theta) sind(theta).*cosd(theta) (cosd(theta)).^2-(sind(
            theta)).^2)];
81
82     Q_bar(:,(i*3-2):i*3) = T\Q*R*T/(R);
83     S_bar(:,(i*3-2):i*3) = inv(Q_bar(:,(i*3-2):i*3));
84
85 end
86
87 % Calculate Z values for plies:
88
89 for i= 1:length(L)+1
90     z(i) = -length(L)/2*t+((i-1)*t);
91 end
92
93 % 2. Calculate ABD matrix and inverse
94
95 A = zeros(3);
96 B = zeros(3);
97 D = zeros(3);
98 ABD = zeros(6);
99
100 for i= 1:3
101     for j= 1:length(L)

```

```

102 A(i,1) = A(i,1)+Q_bar(i,(j*3)-2)*(z(j+1)-z(j));
103 A(i,2) = A(i,2)+Q_bar(i,(j*3)-1)*(z(j+1)-z(j));
104 A(i,3) = A(i,3)+Q_bar(i,(j*3)-0)*(z(j+1)-z(j));
105 B(i,1) = B(i,1)+0.5*(Q_bar(i,(j*3)-2)*(z(j+1)^2-z(j)^2));
106 B(i,2) = B(i,2)+0.5*(Q_bar(i,(j*3)-1)*(z(j+1)^2-z(j)^2));
107 B(i,3) = B(i,3)+0.5*(Q_bar(i,(j*3)-0)*(z(j+1)^2-z(j)^2));
108 D(i,1) = D(i,1)+(1/3)*(Q_bar(i,(j*3)-2)*(z(j+1)^3-z(j)^3));
109 D(i,2) = D(i,2)+(1/3)*(Q_bar(i,(j*3)-1)*(z(j+1)^3-z(j)^3));
110 D(i,3) = D(i,3)+(1/3)*(Q_bar(i,(j*3)-0)*(z(j+1)^3-z(j)^3));
111 end
112 end
113
114 % make values 0 that should be 0:
115 for i= 1:3
116 for j= 1:3
117 if A(i,j) < 1*10^-12 && A(i,j) > -1*10^-12
118 A(i,j) = 0;
119 end
120 if B(i,j) < 1*10^-12 && B(i,j) > -1*10^-12
121 B(i,j) = 0;
122 end
123 if D(i,j) < 1*10^-12 && D(i,j) > -1*10^-12
124 D(i,j) = 0;
125 end
126 end
127 end
128
129 ABD(1:3,1:3) = A;
130 ABD(4:6,1:3) = B;
131 ABD(1:3,4:6) = B;
132 ABD(4:6,4:6) = D;
133 ABDinv = ABD^-1;
134
135 % 3. Apparent laminate stiffness properties:
136 E_x = 1/(length(L)*t*ABDinv(1,1));
137 E_y = 1/(length(L)*t*ABDinv(2,2));
138 v_xy = -ABDinv(1,2)/ABDinv(1,1);
139 G_xy = 1/(length(L)*t*ABDinv(3,3));
140 E_fx = 12/((length(L)*t)^3*ABDinv(4,4));
141 E_fy = 12/((length(L)*t)^3*ABDinv(5,5));
142
143 % 4. Midplane strains and curvatures
144 % Calculate thermal expansion coefficients in x-y:
145 % Calculate N and M thermal
146 alpha = [alpha_1,alpha_2,0]';
147 N_T = [0,0,0]';
148 M_T = [0,0,0]';
149 for i = 1:length(L)
150 theta = L(i);
151
152 T = [(cosd(theta)).^2 (sind(theta)).^2 2*sind(theta).*cosd(theta)
153 (sind(theta)).^2 (cosd(theta)).^2 -2*sind(theta).*cosd(theta)
154 -sind(theta).*cosd(theta) sind(theta).*cosd(theta) (cosd(theta)).^2-(sind(
theta)).^2];

```

```

155 alpha_xy = inv(T)*alpha;
156 Q_bar_T = T\Q*R*T/(R);
157 N_T = N_T+Temp*Q_bar_T*alpha_xy*(z(i+1)-z(i));
158 M_T = M_T+0.5*Temp*Q_bar_T*alpha_xy*(z(i+1)^2-z(i)^2);
159 end
160 N = [N_x,N_y,N_xy]'+N_T;
161 M = [M_x,M_y,M_xy]'+M_T;
162 NM = [N
163 M];
164
165 strain_mid = ABDinv*NM;
166
167 eps_x_mid = strain_mid(1);
168 eps_y_mid = strain_mid(2);
169 eps_xy_mid = strain_mid(3);
170 K_x = strain_mid(4);
171 K_y = strain_mid(5);
172 K_xy = strain_mid(6);
173
174 % 5. Calculation of strains at all points in laminate and plot
175
176 % Calculation of mechanical strain
177 eps_mech_x = eps_x_mid + z*K_x;
178 eps_mech_y = eps_y_mid + z*K_y;
179 eps_mech_xy = eps_xy_mid + z*K_xy;
180
181 eps_mech = [eps_mech_x;eps_mech_y;eps_mech_xy];
182
183 figure(1)
184 plot(eps_mech_x,z,'r-',eps_mech_y,z,'b-',eps_mech_xy,z,'g-')
185 set(gca,'ydir','reverse')
186 legend('\epsilon_x','\epsilon_y','\epsilon_{x-y}')
187 grid on
188 xlabel('Strain, []')
189 ylabel('z,[m]')
190 title('Part 5 - Strain')
191
192 % 6. Calculation of stresses at top and bottom of ply:
193
194 % Get repeating z values at ply interfaces
195 for i=1:length(L)+1
196 zplot((i*2)-1)=z(i);
197 zplot(i*2)=z(i);
198 end
199 zplot(2*(length(L)+1)) = [];
200 zplot(1) = [];
201
202
203 for i = 1:length(L)
204 theta = L(i);
205 T = [(cosd(theta)).^2 (sind(theta)).^2 2*sind(theta).*cosd(theta)
206 (sind(theta)).^2 (cosd(theta)).^2 -2*sind(theta).*cosd(theta)
207 -sind(theta).*cosd(theta) sind(theta).*cosd(theta) (cosd(theta)).^2-(sind(
    theta)).^2];

```

```

208 alpha_xy = inv(T)*alpha;
209 eps_therm = alpha_xy*Temp;
210 eps1 = eps_mech(:,i)-eps_therm;
211 eps2 = eps_mech(:,i+1)-eps_therm;
212 stress_top(:,i) = Q_bar(:,3*i-2:3*i)*(eps1);
213 stress_bottom(:,i) = Q_bar(:,3*i-2:3*i)*(eps2);
214 end
215
216 for i = 1:length(L)
217 stress_xy(:,i*2-1) = stress_top(:,i);
218 stress_xy(:,i*2) = stress_bottom(:,i);
219 end
220
221 % 7. Plots of global stresses for each ply:
222
223 figure(2)
224 plot(stress_xy(1,:),zplot,'-*)
225 legend('\sigma_x')
226 set(gca,'ydir','reverse')
227 grid on
228 xlabel('\sigma_x,[Pa]')
229 ylabel('z,[m]')
230 title('\sigma_x')
231
232 figure(3)
233 plot(stress_xy(2,:),zplot,'-*)
234 legend('\sigma_y')
235 set(gca,'ydir','reverse')
236 grid on
237 xlabel('\sigma_y,[Pa]')
238 ylabel('z,[m]')
239 title('\sigma_y')
240
241 figure(4)
242 plot(stress_xy(3,:),zplot,'-*)
243 legend('\sigma_{x-y}')
244 set(gca,'ydir','reverse')
245 grid on
246 xlabel('\sigma_{x-y},[Pa]')
247 ylabel('z,[m]')
248 title('\sigma_{x-y}')
249
250 % 8. Material coordinates on top and bottom of each ply
251
252 for i = 1:length(L)
253 theta = L(i);
254
255 T = [(cosd(theta)).^2 (sind(theta)).^2 2*sind(theta).*cosd(theta)
256 (sind(theta)).^2 (cosd(theta)).^2 -2*sind(theta).*cosd(theta)
257 -sind(theta).*cosd(theta) sind(theta).*cosd(theta) (cosd(theta)).^2-(sind(
258 theta)).^2];
259
260 alpha_xy = inv(T)*alpha;
261 eps_therm = alpha_xy*Temp;

```



```

261 eps1 = eps_mech(:,i)-eps_therm;
262 eps2 = eps_mech(:,i+1)-eps_therm;
263 stress_top(:,i) = Q_bar(:,3*i-2:3*i)*(eps1);
264 stress_bottom(:,i) = Q_bar(:,3*i-2:3*i)*(eps2);
265 stress_top_12(:,i) = T*stress_top(:,i);
266 stress_bottom_12(:,i) = T*stress_bottom(:,i);
267 end
268
269 for i = 1:length(L)
270 stress_12(:,i*2-1) = stress_top_12(:,i);
271 stress_12(:,i*2) = stress_bottom_12(:,i);
272 end
273
274 % 9. Hashin Failure Criteria:
275
276 Fiber_Failure = ((stress_12(1,:).^2)./(S_L_plus*S_L_minus))+...
277 ((1/S_L_plus-1/S_L_minus).*stress_12(1,:))+...
278 ((stress_12(3,:).^2)./(S_LT^2));
279 Resin_Failure = ((stress_12(2,:).^2)./(S_T_plus*S_T_minus))+...
280 ((1/S_T_plus-1/S_T_minus).*stress_12(2,:))+...
281 ((stress_12(3,:).^2)./(S_LT^2));
282
283 mode = 'No Failure';
284 M=0;
285
286 i = 1;
287 while i <= length(L)
288 theta2((i*2)-1)=L(i);
289 theta2(i*2)=L(i);
290 i = i+1;
291 end
292
293 if max(Fiber_Failure) >= 1
294 mode = 'Fiber Failure';
295 [M, I] = max(Fiber_Failure);
296 z_fail_f = zplot(I);
297 ply_fail_f = theta2(I);
298 end
299 if max(Resin_Failure) >= 1
300 [M2, I2] = max(Resin_Failure);
301 if M2 > M
302 mode = 'Resin Failure';
303 z_fail_r = zplot(I2);
304 ply_fail_r = theta2(I2);
305 end
306 end
307
308 % Outputs to .txt file:
309 i = 1;
310 fid = fopen('outputs_JohnCallaway.txt','wt');
311 fprintf(fid,'John Callaway \n');
312 fprintf(fid,'LPT Code - Spring 2017 \n');
313 fprintf(fid,'\n Part 1 \n');
314 for i = 1:length(L)

```

```

315 fprintf(fid, '\n Ply %i: \n', i);
316 fprintf(fid, '\n The Q matrix is: \n');
317 fprintf(fid, '%8.3g %8.3g %8.3g\n', Q);
318 fprintf(fid, '\n The Q bar Matrix is: \n');
319 fprintf(fid, '%8.3g %8.3g %8.3g\n', Q_bar(:, i*3-2:i*3));
320 fprintf(fid, '\n The S matrix is: \n');
321 fprintf(fid, '%8.3g %8.3g %8.3g\n', S);
322 fprintf(fid, '\n The S bar Matrix is: \n');
323 fprintf(fid, '%8.3g %8.3g %8.3g\n', S_bar(:, i*3-2:i*3));
324 end
325 fprintf(fid, '\n Part 2: \n');
326 fprintf(fid, '\n The ABD matrix is: \n');
327 fprintf(fid, '%8.4g %8.4g %8.4g %8.4g %8.4g %8.4g \n', ABD);
328 fprintf(fid, '\n The ABD inverse matrix is: \n');
329 fprintf(fid, '%8.4g %8.4g %8.4g %8.4g %8.4g %8.4g \n', ABDinv);
330
331 fprintf(fid, '\n Part 3: \n');
332 fprintf(fid, '\n E_x is: \n');
333 fprintf(fid, '%8.2g \n', E_x);
334 fprintf(fid, '\n E_y is: \n');
335 fprintf(fid, '%8.2g \n', E_y);
336 fprintf(fid, '\n v_xy is: \n');
337 fprintf(fid, '%8.2g \n', v_xy);
338 fprintf(fid, '\n G_xy is: \n');
339 fprintf(fid, '%8.2g \n', G_xy);
340 fprintf(fid, '\n E_fx is: \n');
341 fprintf(fid, '%8.2g \n', E_fx);
342 fprintf(fid, '\n E_fy is: \n');
343 fprintf(fid, '%8.2g \n', E_fy);
344
345 fprintf(fid, '\n Part 4: \n');
346 fprintf(fid, '\n Midplane Strain in x is: \n');
347 fprintf(fid, '%8.4g \n', eps_x_mid);
348 fprintf(fid, '\n Midplane Strain in y is: \n');
349 fprintf(fid, '%8.4g \n', eps_y_mid);
350 fprintf(fid, '\n Midplane Strain in xy is: \n');
351 fprintf(fid, '%8.4g \n', eps_xy_mid);
352 fprintf(fid, '\n Curvature in x is: \n');
353 fprintf(fid, '%8.4g \n', K_x);
354 fprintf(fid, '\n Curvature in y is: \n');
355 fprintf(fid, '%8.4g \n', K_y);
356 fprintf(fid, '\n Curvature in xy is: \n');
357 fprintf(fid, '%8.4g \n', K_xy);
358
359 fprintf(fid, '\n Part 6: \n');
360 fprintf(fid, '\n Global Coordinate Stresses: \n');
361 for i = 1:length(L)
362 fprintf(fid, '\n Ply %i Top: ', i);
363 fprintf(fid, ' %8.4g %8.4g %8.4g \n', stress_top(:, i));
364 fprintf(fid, '\n Ply %i Bottom: ', i);
365 fprintf(fid, ' %8.4g %8.4g %8.4g \n', stress_bottom(:, i));
366 end
367
368 fprintf(fid, '\n Part 8: \n');

```

```

369 fprintf(fid, '\n Material Coordinate Stresses: \n');
370 for i = 1:length(L)
371 fprintf(fid, '\n Ply %i Top: ', i);
372 fprintf(fid, ' %8.4g %8.4g %8.4g \n', stress_top_12(:, i));
373 fprintf(fid, '\n Ply %i Bottom: ', i);
374 fprintf(fid, ' %8.4g %8.4g %8.4g \n', stress_bottom_12(:, i));
375 end
376
377 fprintf(fid, '\n Part 9: \n');
378
379 if strcmp(mode, 'No Failure')
380 fprintf(fid, '\n No failure occurred \n');
381 end
382 if strcmp(mode, 'Fiber Failure')
383 fprintf(fid, 'Ply %i failed first, its orientation is %d degrees \n', ceil(I/2),
        ply_fail_f);
384 fprintf(fid, 'The location of the failure is %8.3g m \n', z_fail_f);
385 fprintf(fid, 'The failure occurred in the fibers \n');
386 end
387 if strcmp(mode, 'Resin Failure')
388 fprintf(fid, 'Ply %i failed first, its orientation is %d degrees \n', ceil(I2
        /2), ply_fail_r);
389 fprintf(fid, 'The location of the failure is %8.3g m \n', z_fail_r);
390 fprintf(fid, 'The failure occurred in the resin \n');
391 end

```

8.2 equations

$$[Q] = \begin{bmatrix} \frac{E_1}{1-\nu_{12}\nu_{21}} & \frac{\nu_{12}E_2}{1-\nu_{12}\nu_{21}} & 0 \\ \frac{\nu_{12}E_2}{1-\nu_{12}\nu_{21}} & \frac{E_2}{1-\nu_{12}\nu_{21}} & 0 \\ 0 & 0 & \frac{1}{G_{12}} \end{bmatrix} \quad (1)$$

$$[T] = \begin{bmatrix} \cos^2(\theta) & \sin^2(\theta) & 2\sin(\theta)\cos(\theta) \\ \sin^2(\theta) & \cos^2(\theta) & -2\sin(\theta)\cos(\theta) \\ -\sin(\theta)\cos(\theta) & \sin(\theta)\cos(\theta) & \cos^2(\theta) - \sin^2(\theta) \end{bmatrix} \quad (2)$$

$$[R] = \begin{bmatrix} 1 & 0 & 0 \\ 0 & 1 & 0 \\ 0 & 0 & 2 \end{bmatrix} \quad (3)$$

$$\bar{Q} = T^{-1}QRTR^{-1} \quad (4)$$

$$A_{ij} = \sum_{k=1}^N (\bar{Q}_{ij})_k (z_k - z_{k-1}) \quad (5)$$

$$B_{ij} = \sum_{k=1}^N (\bar{Q}_{ij})_k (z_k^2 - z_{k-1}^2) \quad (6)$$

$$D_{ij} = \sum_{k=1}^N (\bar{Q}_{ij})_k (z_k^3 - z_{k-1}^3) \quad (7)$$

$$\begin{bmatrix} N_x \\ N_y \\ N_{xy} \\ M_x \\ M_y \\ M_{xy} \end{bmatrix} = \begin{bmatrix} A_{11} & A_{12} & A_{16} & B_{11} & B_{12} & B_{16} \\ A_{21} & A_{22} & A_{26} & B_{21} & B_{22} & B_{26} \\ A_{61} & A_{62} & A_{66} & B_{61} & B_{62} & B_{66} \\ B_{11} & B_{12} & B_{16} & D_{11} & D_{12} & D_{16} \\ B_{21} & B_{22} & B_{26} & D_{21} & D_{22} & D_{26} \\ B_{61} & B_{62} & B_{66} & D_{61} & D_{62} & D_{66} \end{bmatrix} \begin{bmatrix} \epsilon_x \\ \epsilon_y \\ \epsilon_{xy} \\ \kappa_x \\ \kappa_y \\ \kappa_{xy} \end{bmatrix} \quad (8)$$

$$\gamma_{xy} = 2\epsilon_{OB} - (\epsilon_x + \epsilon_y) \quad (9)$$

$$\epsilon = \frac{-2V_r}{GF[(v+1) - V_r(v-1)]} \quad (10)$$

$$V_R = \frac{V_{CH} - V_0}{V_{EX} Gain} \quad (11)$$

$$Gain = \frac{5}{(\frac{V_{EX}}{1000}) R_{shunt}} \quad (12)$$

$$M = \frac{3PL}{10} \quad (13)$$